Novel fluorescent probe for sequential recognition of Zn^{2+} and pyrophosphate in aqueous based on aggregation-induced emission

Qinghong Bai [a #], Yu Xia [b #], Guangyan Liang[b], Chenhui Wang [a], Carl Redshaw [c], Xin Xiao[a*]

[a] Key Laboratory of Macrocyclic and Supramolecular Chemistry of Guizhou Province, Guizhou University, Guiyang 550025, China
[b] The Key Laboratory of Chemistry for Natural Products of Guizhou Province and Chinese Academy of Sciences, Guiyang 550014, PR China
[c] Chemistry, School of Natural Sciences, University of Hull, Hull HU6 7RX, U.K.
[#]These authors contributed equally to this work.

Abstract

A new fluorescent probe (E)-4-(4-([2,2':6',2"-terpyridin]-4'-yl)styryl)-1-dodecylpyridin-1-ium (**TPy-SD**), with the aggregation-induced emission (AIE) property in aqueous solution, has been characterized. The new probe, **TPy-SD** exhibited excellent selectivity and sensitivity towards Zn^{2+} with a relatively low detection limit (1.76 $x10^{-7}$ M). The addition of Zn^{2+} is thought to disrupt the AIE property of **TPy-SD**, thereby leading to a fluorescence blue shift. Interestingly, the complex of probe **TPy-SD** with Zn^{2+} (**Zn (II) TPy-SD**), with molar ratio of 1:1, can be used as a simple, sensitive, and rapid means for the detection of pyrophosphates (PPi) in solution (water/DMSO = 99:1). As evidenced by transmission electron microscopy (TEM), dynamic light scattering (DLS) and fluorescence emission spectroscopy, this detection is thought to be due to the strong affinity between PPi and Zn^{2+}, which brings out Zn^{2+} from the coordination cavity of chemical sensor **TPy-SD**, thus realizing the detection and recognition of PPi. Therefore, the new AIE fluorescent probe can be used as a dual probe for the detection of cations and anions.

Keywords: Fluorescent probe; Zn^{2+}; PPi; Aggregation-induced emission (AIE).

Introduction

Over the past decade, the study of molecules exhibiting the aggregation-induced emission (AIE) effect has received much attention due to their enhanced luminescence when aggregated or in the solid state [1-5]. In addition, compared with monomeric organic compounds as chemical probes, aggregated organic compounds tend to have higher selectivity and sensitivity toward metal ions [6,7]. Terpyridine (TPy), one of the most studied AIE luminescent systems, has been widely used in chemical sensors and biological probes because of its simple preparation and facile functionalization [8-10]. More importantly, tripyridine and its derivatives have been well-studied as ligands for transition metal ions, and produce highly stable complexes with attractive optical, electronic and magnetic properties [11,12]. This has opened up a new pathway in the field of coordination and supramolecular chemistry [13], particularly in the case of ion selective chemical probes constructed using aggregated ligation.

Zinc is one of the most abundant trace elements in the human body, and plays an important role in many biological processes [14], such as gene expression, cell metabolism, neurotransmission and apoptosis [15-18]. Hence, the identification and detection of Zn^{2+} ions is of great significance for understanding the pathophysiological homeostasis and biological processes in the human body. To date, numerous fluorescent chemical sensors for Zn^{2+} have been designed and developed [19-22], but there are limitations such as complex multistep syntheses, insufficient selectivity and/or sensitivity. Therefore, the development of water-soluble zinc sensors that are easy to prepare with improved sensitivity and selectivity will continue to be an area of interest [23,24].

Pyrophosphate (PPi) is an important anion, not only because it plays an important role in a wide range of key biological processes, but also because it is widely used in various industrial applications [25]. It is known that PPi, as the product of ATP hydrolysis under cellular conditions, participates in biological processes such as cellular signal transduction, gene transcription and protein synthesis [14]. Also, PPi is the most common cause of eutrophication in industry and has attracted great attention because of its use as a new negative electrode material for lithium batteries, and has been recognized as an effective catalyst for *n*-butane oxidation to maleic anhydride [26]. Given this, the

identification and detection of PPi has attracted increased attention from the research community. However, it remains a challenging task to design water-soluble fluorescent chemosensors for the selective detection of PPi in aqueous media because of the high solvation energy of PPi in water (DG0 = 584 KJ/moL) [27] and the existence of other competitive anions.

In recent years, metal ion complexes have been used to develop fluorescent phosphate sensors due to the special interaction between metal ions and anions [28-30]. However, instances of specific identification and quantitative detection of PPi and other phosphate anions in aqueous media remain somewhat limited. Therefore, there is a great demand for the development of highly efficient PPi optical chemical sensors which can work in water. TPy derivatives, especially those substituted at the 4'-position, are readily available [31]. Moreover, due to the rotational arrangement of the ring nitrogens, TPy derivatives can efficiently coordinate with transition metals [32-34].

Herein, we have designed a new AIE fluorescent probe (E)-4-(4-([2,2':6',2''-terpyridin]-4'-yl)styryl)-1-dodecylpyridin-1-ium (**TPy-SD**) based on a tripyridine derivative, which shows excellent selectivity and sensitivity towards Zn^{2+} with a relatively low detection limit in aqueous media. Interestingly, the complex **Zn(II)TPy-SD** can be used as a simple, sensitive, and rapid means for the detection of pyrophosphates (PPi) in aqueous medium. The advantage of this recognition is that it can effectively eliminate the interference caused by other competitive anions and solvent molecules due to the metal coordination effect [35-37].

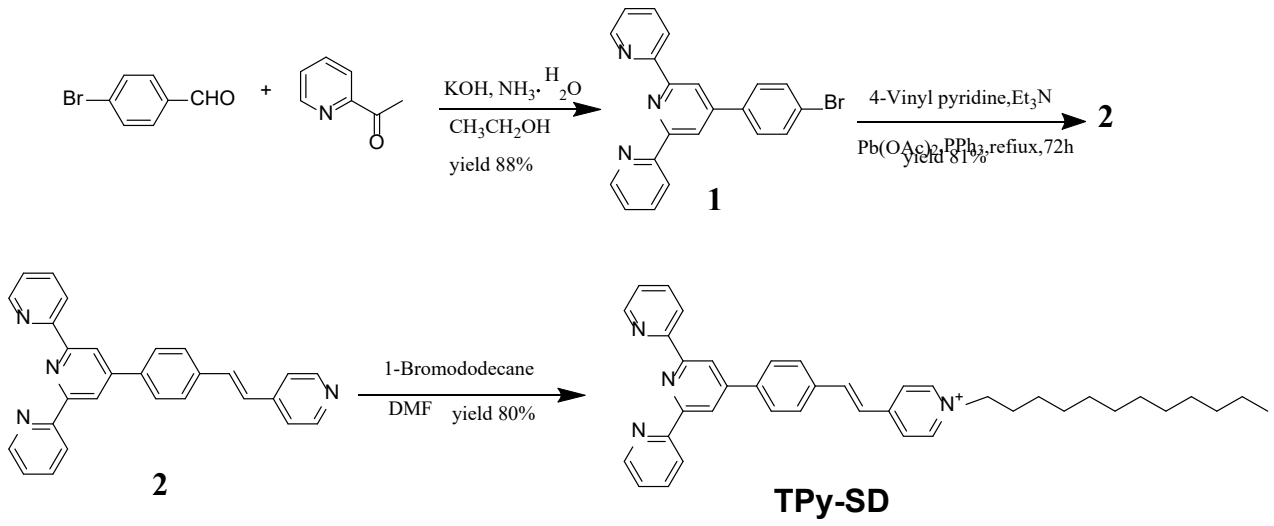

Scheme 1. Synthesis of probe **TPy-SD**.

Materials and Methods

2.1. Materials

The reagents were purchased from the Shanghai Aladdin Biochemical Technology Co., Ltd. and were used as received. Anions (ClO_4^- , Br^-, Cl^-, F^-, NO_3^-, SO_4^{2-}, $H_2PO_4^-$, I^-, CO_3^{2-}, AC^-, ADP, ATP) were used as sodium or potassium salts, and cations as perchlorate salts (Zn^{2+}, Hg^{2+}, Ca^{2+}, Fe^{2+}, Fe^{3+}, Mn^{2+}, Ba^{2+}, Na^+, Ni^{2+}, K^+, Mg^{2+}, Al^{3+}, Li^+, Cu^{2+}, Pb^{2+}, Co^{2+}, Cd^{2+}).

2.2. Instruments and measurements

A Varian Cary Eclipse fluorescence spectrophotometer was used to record the fluorescence emission spectrum of the host-guest complexes. ^1H NMR spectra were measured on a Nippon Denshi JEOL FT-400 NMR spectrometer with Me_4Si as an internal reference. Transmission electron microscopy (TEM) experiments were performed on a Hitachi JEM-2100 TEM. Samples were prepared by carefully dropping a solution of the sample onto a carbon-coated copper grid and then removing the solvent by air drying. DLS was performed on a laser light scattering spectrometer (BI-200SM) equipped with a digital correlator (BI-9000AT) at λ = 514 nm under room temperature conditions. Mass spectra were obtained by Thermos Q Exactive Focus.

2.3. Methods

The stock solutions for the fluorescence emission studies of **TPy-SD** (1.00×10^{-3} $mol\cdot L^{-1}$) were prepared in dimethyl sulfoxide (DMSO). Stock solutions (1.00×10^{-2} $mol\cdot L^{-1}$) of different cations and anions in deionized water were also prepared. The fluorescence spectra of the host-guest complexes were recorded at 25 °C. Working solutions were prepared by diluting the stock solutions to the required concentrations. A solution of the **TPy-SD** and Zn^{2+} (1:1) complex was prepared at a fixed concentration of 1×10^{-5} $mol\cdot L^{-1}$ in solution (water/DMSO = 99:1). Fluorescence spectra were obtained at an excitation of 351 nm (emission and excitation bandwidths: 10 nm). For each experiment, three replicate measurements were recorded.

Limit of detection (LOD) measurement

The LOD was calculated based on the standard derivation (σ) of 10 measurements without guest molecules and the slope (K) of a linear calibration curve with the formula LOD=3σ/K. The standard deviation formula for 10 measurements in the absence of guest molecules was formulated as: $\sqrt{\frac{1}{n-1}\sum_{i=1}^{n}(x_i - \bar{x})^2} \quad (n = 11)$

2.3 Synthesis and structural characterization of the probe TPy-SD

Compound 1. The probe **TPy-SD** was synthesized according to the synthetic route shown in Scheme 1. Compounds **1** and **2** were synthesized by a previously reported literature method [38]. A mixture of 4-bromobenzaldehyde (2 g, 10.9 mmol), 2-acetylpyridine (2.42 g, 20 mmol), potassium hydroxide (1.7 g), 29 mL ammonia and 50 ml ethanol was added to a 150 ml round-bottomed flask. The mixture was stirred for 1 h at 0 ℃, then refluxed for one day, and stirred at room temperature for 1 h. The precipitate was filtered off, and recrystallized twice with ethanol to obtain compound **1**. Yield: 88%. ^{1}H NMR (400 MHz, DMSO-d_6): δ 8.77 – 8.75 (m, 2H), 8.69 (s, 2H), 8.66 (d, J = 7.9 Hz, 2H), 8.03 (td, J = 7.7, 1.8 Hz, 2H), 7.89 (d, J = 8.5 Hz, 2H), 7.77 (d, J = 8.5 Hz, 2H), 7.53 (ddd, J = 7.5, 4.7, 1.1 Hz, 2H).

Compound 2. A mixture of compound **1** (500 mg, 1.3 mmol), 4-vinyl pyridine (150 mg), palladium acetate (30 mg, 0.13 mmol), triphenylphosphine (102 mg, 0.4 mmol) and triethylamine (10 mL) was added to a high-pressure reaction flask under nitrogen atmosphere, and then refluxed at 120 ℃ for 72 h. After the reaction, the mixture was cooled to room temperature, extracted into CH_2Cl_2, and washed three times each with distilled water and saturated salt solution. The organic reagent was removed by rotary evaporation, the crude product was dissolved in dichloromethane, and compound **2** was obtained by recrystallization from ethanol yield: 81%.^{1}H NMR (400 MHz, DMSO-d_6): δ 8.77 (d, J=4.0 Hz, 2H), 8.75 (s, 2H), 8.68 (d, J=8.0 Hz, 2H), 8.57 (d, J=6.0 Hz, 2H), 8.05 (td, J=7.6, 1.6 Hz, 2H), 8.0 (d, J=8.4 Hz, 2H), 7.8 (d, J=8.4 Hz, 2H), 7.66 (d, J=16.4 Hz, 1H), 7.62 (d, J=6.0 Hz, 2H), 7.54 (ddd, J = 6.8, 5.2, 0.8 Hz, 2H), 7.39 (d, J=16.4 Hz, 1H).

Compound TPy-SD. A mixture of compound **2** (0.5 mmol), DMF (5 mL) and 1-

bromododecane (1 mmol) was added into a 10 mL round bottom flask, and stirred continuously for 24 h at 80 ℃. After the reaction, the mixture was cooled to room temperature, and then 30 mL diethyl ether was added to the filtrate to obtain a yellow precipitate. Following filtration, the crude product was washed three times with diethyl ether, and dried to afford the compound **TPy-SD** Yield: 80%.^{1}H NMR (400 MHz, DMSO-d_6) : δ 8.94 (d, J = 6.7 Hz, 2H), 8.75 (m, 4H), 8.67 (d, J = 7.9 Hz, 2H), 8.26 (d, J = 6.7 Hz, 2H), 8.12 - 8.10 (m, 2H), 7.93 (d, J = 8.4 Hz, 2H), 8.08 (td, J = 8.0Hz, 2H),7.63 (d, J = 16.3 Hz, 2H), 7.57 - 7.48 (m, 2H), 4.46 (t, J = 7.3 Hz, 2H),1.87 (s, 2H), 1.24-1.15 (m, 18H), 0.80 (s, 3H). ^{13}C NMR (100 MHz, DMSO-d_6), δ 156.32, 149.83, 144.79, 140.35, 138.00, 129.58, 128.10, 124.68, 124.53, 60.28, 40.35, 40.21, 40.07, 39.94, 39.80, 39.68, 39.59, 31.76, 31.00, 29.31, 28.85, 25.88, 22.55, 14.42. Mp. 25°C. MS m/z: calcd for $C_{40}H_{45}N_4^+$: 581.36; found: 581.36.

Results and discussion

As shown in Scheme 1, **TPy-SD** was synthesized from commercially available chemicals via several steps. In the experimental section, the synthetic route and structure characterization of **TPy-SD** (Fig. S1–S3) are described in detail.

From a structural perspective, the tripyridine skeleton endows the styrylpyridine with typical AIE characteristics [39]. In other words, in a good solvent, the C-C bond between the three pyridine rings and the C-C bond between the tripyridine and styrylpyridine can rotate freely, which reduces the planarity of the molecule, with the result that the fluorophore has weak or no emission. In a solvent with poor solubility, the intramolecular motions are restricted, blocking the nonradiative decay channels, making the fluorophore molecules highly luminous [40]. In order to understand the AIE behavior of **TPy-SD** in solution, the fluorescence spectra of **TPy-SD** in different solvents were first evaluated. As shown in Fig.1a, in common organic solvents, **TPy-SD** exhibited the typical blue emission of styrenyl pyridine at 450 nm. This result indicated that **TPy-SD** has good solubility in these solutions and therefore produced monomer emission. Surprisingly, the fluorescence of **TPy-SD** was enhanced and a yellow emission spectrum appeared in aqueous solution, which caused the AIE phenomenon. To further prove the

AIE effect of **TPy-SD**, the fluorescence spectrum of the probe was studied in a DMSO/H_2O system. In general, when an appropriate amount of non-solvent was added, aggregates can form, and this is a common method for estimating the AIE behavior in solvent/non-solvent mixtures [41]. As shown in Fig.1b, **TPy-SD** emitted weak blue fluorescence in DMSO solution, which may be attributed to the rotation of multiple pyridine ring active molecules that consumed the excited state energy and resulted in the weakening of fluorescence. Due to the distortion of the charge transfer process in the probe molecule, the fluorescence gradually decreases with the increase of water volume ratio. When f_w > 60%, the excited state decayed to the corresponding ground state through strong fluorescence emission, and when the content of water increased, the maximum emission wavelength changed from 450 nm to 545 nm (Fig.1b and c), which was mainly due to aggregate-induced π-π interactions between the adjacent terpyridine of **TPy-SD** [42]. Under a UV lamp, the color changed from blue to bright yellow (Fig.1d). These results further indicated that **TPy-SD** was AIE-active.

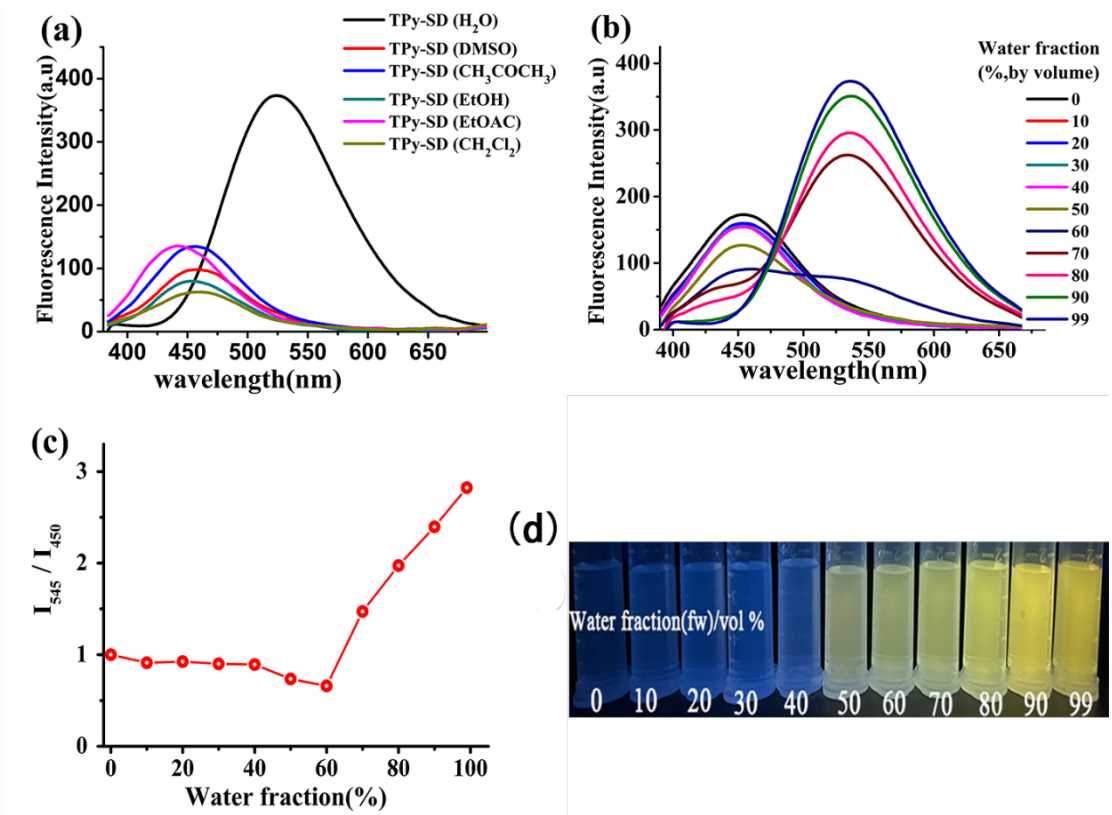

Figure 1. (a) Fluorescence spectra of probe **TPy-SD** in several organic reagents and aqueous solutions; (b) Fluorescence spectra of **TPy-SD** (10 μM) in the DMSO/H_2O system with different water fraction (f_w) excited at 351 nm; (c) Plot of the changes of the peak fluorescence spectra intensity of **TPy-SD** with variation of f_w; (d) Photograph of DMSO/water mixture solution of **TPy-SD** under UV light at 365 nm.

Fig. 2a,b shows the fluorescence of aggregate-based **TPy-SD** and its response towards various metal ions in solution (water/DMSO = 99:1). There was no significant change in the fluorescence spectrum upon the addition of other metal ions, including Cd^{2+} or the VIIIA metal ions (Fe^{2+}, Fe^{3+}, Co^{2+} and Ni^{2+}). However, under the same experimental conditions, when Zn^{2+} was added, the fluorescence spectrum showed a significant blue shift, and the maximum emission spectrum was shifted from 545 nm to 450 nm. Under UV light, the fluorescent color changed from yellow to blue (Fig. 2c). These results indicate that **TPy-SD** exhibits high selectivity for Zn^{2+} in aqueous solution.

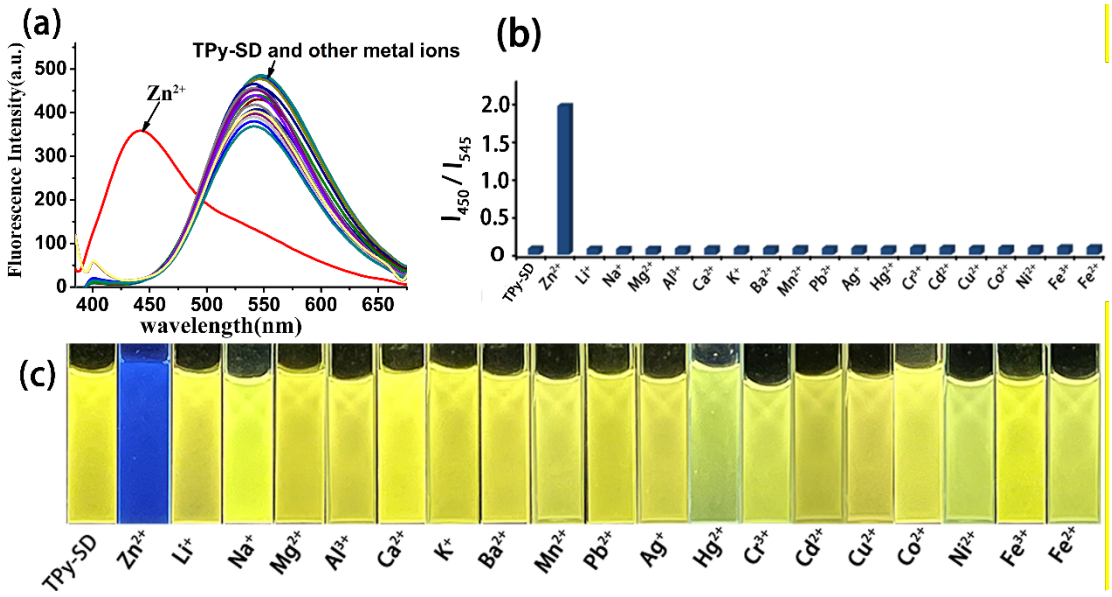

Figure 2. (a) Fluorescence spectra of **TPy-SD** (10.0 μM) in solution (water/DMSO = 99:1) at room temperature upon addition of various metal ions (50.0 μM); (b) Relative fluorescence intensity changes; (c) Photographs of the aqueous solution of **TPy-SD** in the presence of various metal ions (50.0 μM) under UV light at 365 nm.

The effect of different concentrations of Zn^{2+} on the probe **TPy-SD** was also investigated. As shown in the Fig. 3a, on increasing the concentration of Zn^{2+}, the fluorescence intensity at 545 nm gradually decreased, and at 450 nm was obviously enhanced. From the fluorescence titration spectral data, the binding constant (Ka) of probe **TPy-SD** to Zn^{2+} was calculated at 1.04 $\times 10^5$ M^{-1} (Fig. S4 and Table S1). Over a certain concentration range, the fluorescence intensity has a good linear relationship with [Zn^{2+}]. From the plot in Fig. S5 and Table S2, the detection limit of Zn^{2+} (LOD) was calculated at 1.76 x10^{-7} M. Moreover, the combined stoichiometric ratio of **TPy-SD** and Zn^{2+} was determined to be 1:1 by a Job's plot (Fig. 3b). In addition, in order to further

evaluate the analytical application of the probe to target metal ions in aqueous solution, the interference of the probe's selective response to Zn^{2+} in the presence of other metal ions was evaluated. The fluorescence intensity was almost the same as that without other cations, which reflected that coexisting ions did not interfere with the recognition of **TPy-SD** when detecting Zn^{2+} (Fig. S6). Compared with other AIE probes which have been reported for the recognition of zinc ions in recent years [43-47], the **TPy-SD** probe has better water solubility and a lower detection limit (Table 1). These results indicate that the probe **TPy-SD** has advantages in selectivity and sensitivity toward zinc ions.

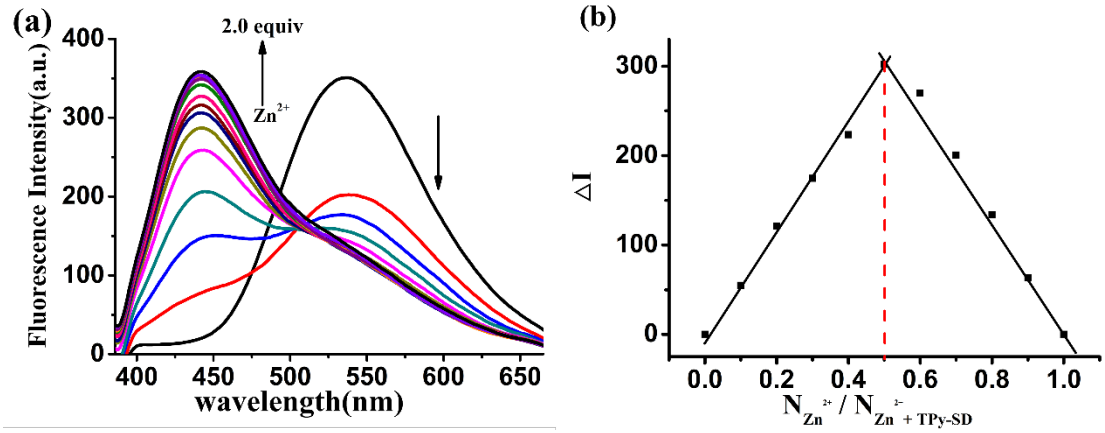

Figure 3. (a) Fluorescence spectra of **TPy-SD** (1×10^{-5} mol·L^{-1}) with increasing molar equivalents of Zn^{2+} from 0, 0.1, 0.2, 0.3, 0.4, 0.5, 0.6… to 2.0; (b) Job's plot for Zn^{2+} with **TPy-SD**.

Table 1. Comparison of the solvents and detection limits (LOD) with recently reported AIE probes for Zn^{2+}

Solvents	LOD (M)	Reference
THF	1.24×10^{-6}	43
C_2H_5OH	3.02×10^{-7}	44
DMSO / H_2O (9:1, v/v)	3.65×10^{-6}	45
H_2O / THF (9:1, v/v)	3.7×10^{-7}	46
DMF / H_2O (2:3, v/v)	2.5×10^{-7}	47
H_2O / DMSO (99:1, v/v)	1.76×10^{-7}	This work

To obtain more information on the interaction of the probe with the cation, transmission electron microscopy (TEM) and dynamic light scattering (DLS) experiments were performed. As shown in Fig. S7a, in solution (water/DMSO = 99:1), the transmission electron microscopy (TEM) experiment showed that the newly prepared probe **TPy-SD** exhibited a large number of distorted bands, and the structure became spherical after standing for 12 h (Fig. S7b). This result further supported the statement that **TPy-SD** exhibited an aggregation-induced emission enhancement effect. However, when Zn^{2+} was added, the structure became fragmented (Fig. S7c), after 12 h, it was also fragmented (Fig. S7d). Thus, we hypothesized that the fluorescence blue shift was caused by metal coordination to trigger the disassembly of **TPy-SD**. As shown in Fig. 4 and Fig. S8, the DLS revealed that the average particle size of the newly prepared **TPy-SD** solution was 225.9 nm and that of the solution placed for 12 h was 896.5 nm, while the average particle size of the **TPy-SD** with Zn^{2+} was 18.5 nm. When a beam of light passed through the solution of **TPy-SD** without Zn^{2+}, a bright "path" could be observed; for the solution with Zn^{2+} this was not the case. This result further supported our conjecture that the disassembly of **TPy-SD** was triggered by the coordination of metal ions, which results in a blue shift of fluorescence.

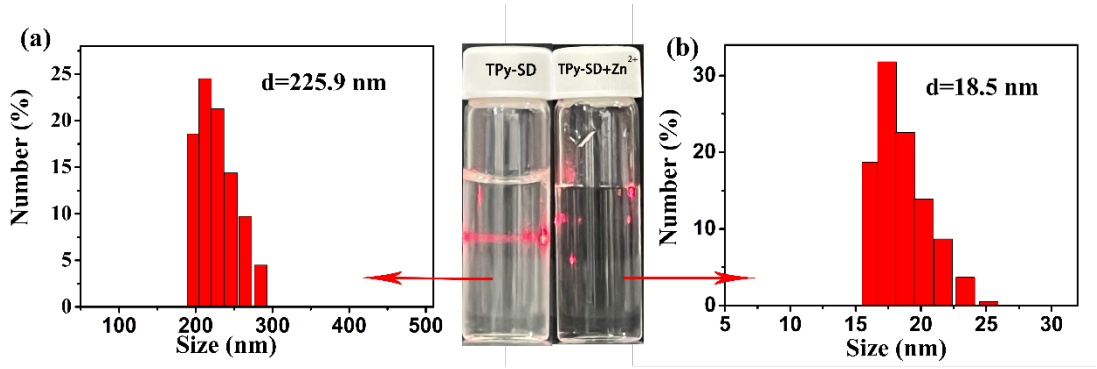

Figure 4. (a) DLS data of the newly prepared **TPy-SD** (10.0 μM) and (b) DLS data of **TPy-SD** (10.0 μM) in the presence of Zn^{2+} (50.0 μM) in solution (water/DMSO = 99:1) and photograph of a Tyndall effect in day light.

In recent years, metal ion complexes have been used as sensor for anions. Therefore, we investigated whether the complex of probe **TPy-SD** with Zn^{2+} (**Zn (II) TPy-SD**), with the molar ratio 1:1, could be used as a fluorescent probe to detect and recognize

anions. Interestingly, when different anions, such as ClO_4^- , Br^-, Cl^-, F^-, NO_3^-, SO_4^{2-}, $H_2PO_4^-$, I^-, CO_3^{2-}, AC^-, ADP, ATP were added, the fluorescence of probe **Zn (II) TPy-SD** did not change. Whereas in the presence of PPi, the maximum emission peak of the probe **Zn (II) TPy-SD** was red-shifted from 450 nm to 545 nm and the fluorescence intensity was clearly enhanced. Under ultraviolet light, the fluorescent color changed from blue to yellow (Fig.5a). This result indicated that the probe **Zn (II) TPy-SD** could recognize PPi with high selectivity in solution (water/DMSO = 99:1). In order to obtain more information about the probe **Zn (II) TPy-SD** and PPi, titration experiments were conducted. As shown in Fig. 5b, on increased addition of PPi (0-5 equiv.), the fluorescence intensity of the probe gradually decreased at 450 nm and increased at 545 nm. Over a certain concentration range, probe **Zn (II) TPy-SD** exhibited a good linear relationship with PPi. As shown in Fig. S9 and Table S3, the detection limit (LOD) of PPi was calculated at 4.88 x 10^{-7} M. In order to further evaluate the utility of **Zn (II) TPy-SD** as an anion-selective probe, the fluorescence emission changes of **Zn (II) TPy-SD** after the addition of other anions in the presence of PPi were investigated. As we expected, the results showed that the fluorescence emission spectra of **Zn (II) TPy-SD** to other anions were almost unchanged in the presence of PPi anions (Fig. S10). Therefore, it can be concluded that the above anions, except for PPi, did not affect the emission characteristics of **Zn (II) TPy-SD**, indicating that **Zn (II) TPy-SD** can be used as a sensing molecular system for a rapid selective response to PPi.

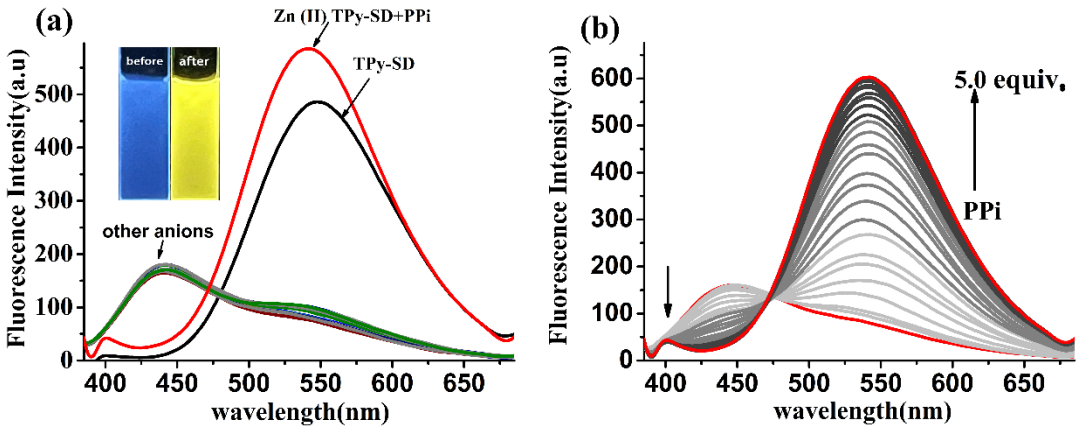

Figure 5. (a) Fluorescence spectra of **Zn (II) TPy-SD** (10.0 μM) in the presence of various anions (each of 50.0 μM) in solution (water/DMSO = 99:1); (b) Fluorescence spectra of **Zn (II) TPy-SD** upon addition of increasing concentrations of PPi in solution (water/DMSO = 99:1).

Among the phosphates, PPi has a high affinity toward Zn^{2+} [48]. Here, the strong interaction between Zn^{2+} and PPi can promote the rupture of the **Zn (II) TPy-SD** complex, thus restoring the probe **TPy-SD** to its original spectral position (545 nm) in solution (water/DMSO = 99:1). To achieve a further understanding of the assembly controlled by PPi, transmission electron microscopy (TEM) and dynamic light scattering (DLS) experiments were performed. As shown in Fig. 6a, the structure of **TPy-SD** with PPi revealed twisted bands in the TEM images, which was similar to the TEM images of the newly prepared probe **TPy-SD**. The DLS data showed that the average particle size of **Zn (II) TPy-SD** with PPi was 238.9 nm in solution (water/DMSO=99:1) and a Tyndall effect was observed when the solution of **Zn (II) TPy-SD** in the presence of PPi was irradiated with a laser pointer in day light (Fig. 6b). These results indicated that the probe has reaggregated.

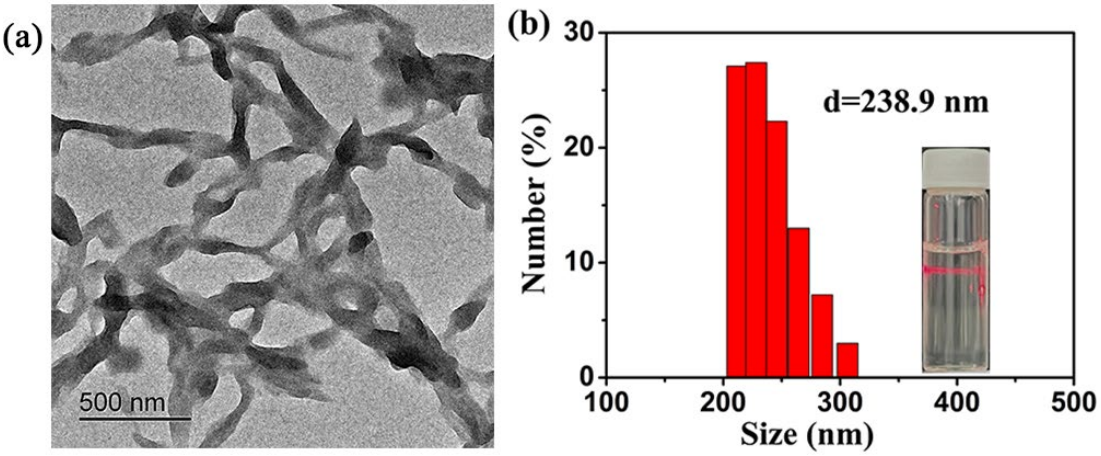

Figure 6. (a) TEM image of **Zn (II) TPy-SD** (10.0 μM) in the presence of PPi (50.0 μM) in solution (water/DMSO = 99:1); (b) DLS data of **Zn (II) TPy-SD** (10.0 μM) in the presence of PPi (50.0 μM) in solution (water/DMSO = 99:1) and photograph of a Tyndall effect in day light.

Conclusion

A novel AIE fluorescent probe based on a styrylpyridinium attached to a terpyridine fluorophore was synthesized and characterized. Complex **TPy-SD** showed excellent sensitivity and selectivity for Zn^{2+} with a low detection limit in solution

(water/DMSO = 99:1). Whereas the zinc-bound adduct (**Zn (II) TPy-SD**) was found to have the ability to recognize PPi without interference from common anions, enabling it to be used as a dual probe for the detection of cations and anions. As evidenced by TME and DLS and emission spectroscopy, the probe **TPy-SD** formed a 1:1 complex with Zn^{2+}, which induced the disassembly of **TPy-SD**, thereby creating the fluorescence blue shift. On subsequent addition of PPi, the maximum emission spectrum red-shifted to the original position. This is thought to be due to the strong affinity between PPi and Zn^{2+}, which brings out Zn^{2+} from the coordination cavity of chemical sensor **TPy-SD**, thus realizing the detection and recognition of PPi（Fig. 7). The present work provides a new approach to expand the application of AIE fluorescent probes, which can be used as dual probes for the detection of both cations and anions.

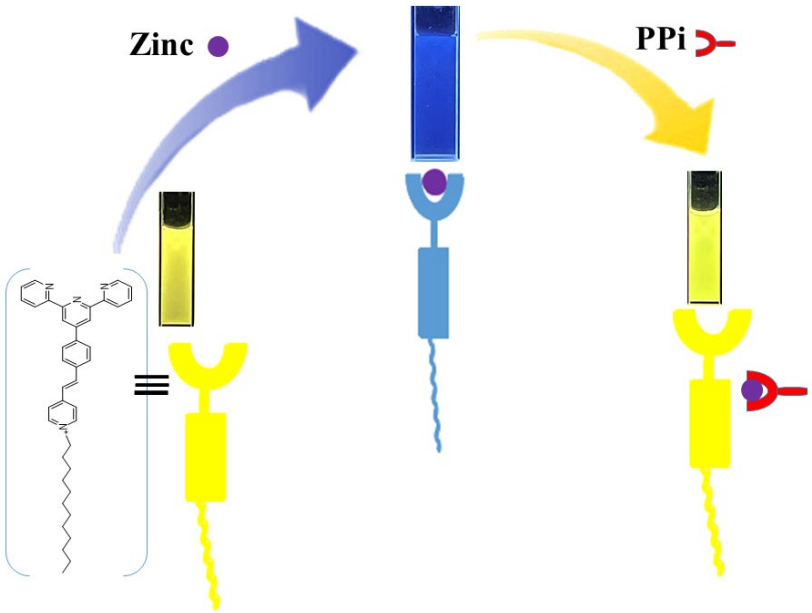

Figure 7. Schematic diagram of the probe **TPy-SD** for detecting and identifying Zn^{2+} and PPi in solution (water/DMSO = 99:1)

Acknowledgments

This work was financially supported by the Science and Technology Fund of Guizhou Province. CR thanks the University of Hull for support.

Conflict of Interest

There is no conflict of interest.

References

(1) Singh, V. D.; Singh, R. S.; Paitandi, R. P.; Dwivedi, B. K.; Maiti, B.; Pandey, D. S. Solvent-Dependent Self-Assembly and Aggregation-Induced Emission in Zn(II) Complexes Containing Phenothiazine-Based Terpyridine Ligand and Its Efficacy in Pyrophosphate Sensing. *The Journal of Physical Chemistry C* **2018,** *122* (9), 5178.

(2) Jiang, G.; Yu, J.; Wang, J.; Tang, B. Z. Ion–π interactions for constructing organic luminescent materials. *Aggregate* **2022,** *3* (6).

(3) Jiang, G.; Hu, R.; Li, C.; Gong, J.; Wang, J.; Lam, J. W. Y.; Qin, A.; Zhong Tang, B. Dipole-Dipole and Anion-pi(+) Interaction Manipulation Synergistically Enhance Intrinsic Antibacterial Activities of AIEgens. *Chemistry* **2022,** *28* (63), e202202388.

(4) Yu, J.; Jiang, G.; Wang, J. In Vivo Fluorescence Imaging-Guided Development of Near-Infrared AIEgens. *Chem Asian J* **2023**, DOI:10.1002/asia.202201251 10.1002/asia.202201251, e202201251.

(5) Zuo, M.; Qian, W.; Hao, M.; Wang, K.; Hu, X.-Y.; Wang, L. An AIE singlet oxygen generation system based on supramolecular strategy. *Chinese Chemical Letters* **2021,** *32* (4), 1381.

(6) Jung, S. H.; Kwon, K. Y.; Jung, J. H. A turn-on fluorogenic Zn(II) chemoprobe based on a terpyridine derivative with aggregation-induced emission (AIE) effects through nanofiber aggregation into spherical aggregates. *Chem Commun (Camb)* **2015,** *51* (5), 952.

(7) Liu, N.; Chen, Z.; Fan, W.; Su, J.; Lin, T.; Xiao, S.; Meng, J.; He, J.; Vittal, J. J.; Jiang, J. Highly Efficient Multiphoton Absorption of Zinc-AIEgen Metal-Organic Frameworks. *Angew Chem Int Ed Engl* **2022,** *61* (12), e202115205.

(8) Divya, V.; Sankar, V.; Raghu, K. G.; Reddy, M. L. A mitochondria-specific visible-light sensitized europium beta-diketonate complex with red emission. *Dalton Trans* **2013,** *42* (34), 12317.

(9) Fermi, A.; Bergamini, G.; Roy, M.; Gingras, M.; Ceroni, P. Turn-on phosphorescence by metal coordination to a multivalent terpyridine ligand: a new paradigm for luminescent sensors. *J Am Chem Soc* **2014,** *136* (17), 6395.

(10) Cheng, M.; Jiang, J.; Chambron, J.-C.; Wang, L. High-resolution and instantaneous imaging of latent fingerprints. *Chinese Chemical Letters* **2023,** *34* (4).

(11) Long, D. L.; Burkholder, E.; Cronin, L. Polyoxometalate clusters, nanostructures and materials: from self assembly to designer materials and devices. *Chem Soc Rev* **2007,** *36* (1), 105.

(12) Wild, A.; Winter, A.; Schlutter, F.; Schubert, U. S. Advances in the field of pi-conjugated 2,2':6',2"-terpyridines. *Chem Soc Rev* **2011,** *40* (3), 1459.

(13) Yamaki, Y.; Nakamura, T.; Suzuki, S.; Yamamura, M.; Minoura, M.; Nabeshima, T. A Self-Assembled Rectangular Host with Terpyridine-Platinum(II) Moieties That Binds Unsubstituted Pentacene in Solution. *European Journal of Organic Chemistry* **2016,** *2016* (9), 1678.

(14) Dong, Z. M.; Wang, W.; Qin, L. Y.; Feng, J.; Wang, J. N.; Wang, Y. Novel reversible fluorescent probe for relay recognition of Zn2+ and PPi in aqueous medium and living cells. *Journal of Photochemistry and Photobiology A: Chemistry* **2017,** *335*, 1.

(15) Malavolta, E. M. M. Zinc Dyshomeostasis, Ageing and Neurodegeneration: Implications of A2M and Inflammatory Gene Polymorphisms. *Alzheimer's Disease 12 (2007) 101–109* **2007**, 101.

(16) Xie, Z.; Wu, H.; Zhao, J. Multifunctional roles of zinc in Alzheimer's disease. *Neurotoxicology* **2020,** *80*, 112.

(17) Masanta, G.; Lim, C. S.; Kim, H. J.; Han, J. H.; Kim, H. M.; Cho, B. R. A mitochondrial-targeted two-photon probe for zinc ion. *J Am Chem Soc* **2011,** *133* (15), 5698.

(18) Lee, N.; Ly, N. H.; Kim, J. S.; Jung, H. S.; Joo, S.-W. A selective triarylmethine-based spectroscopic probe for Zn2+ ion monitoring. *Dyes and Pigments* **2019,** *171*.

(19) Xu, T.; Li, D.; Yan, C.; Wu, Y.; Yuan, C. S.; Shao, X. Decoration of Terpyridine with Electron‐Rich Unit THDTAP: an Efficient Way to Explore Fluorescence Sensors for Recognizing Metal Ions. *Chinese Journal of Chemistry* **2019,** *37* (9), 909.

(20) Hong, Y.; Chen, S.; Leung, C. W.; Lam, J. W.; Liu, J.; Tseng, N. W.; Kwok, R. T.; Yu, Y.; Wang, Z.; Tang, B. Z. Fluorogenic Zn(II) and chromogenic Fe(II) sensors based on terpyridine-substituted tetraphenylethenes with aggregation-induced emission characteristics. *ACS Appl Mater Interfaces* **2011,** *3* (9), 3411.

(21) Bhowmik, S.; Ghosh, B. N.; Marjomaki, V.; Rissanen, K. Nanomolar pyrophosphate detection in water and in a self-assembled hydrogel of a simple terpyridine-Zn2+ complex. *J Am Chem Soc* **2014,** *136* (15), 5543.

(22) Zhou, Y.; Yang, L.; Ma, L.; Han, Y.; Yan, C. G.; Yao, Y. Nano-Theranostics Constructed from Terpyridine-Modified Pillar [5]arene-Based Supramolecular Amphiphile and Its Application in Both Cell Imaging and Cancer Therapy. *Molecules* **2022,** *27* (19).

(23) Chettri, B.; Jha, S.; Dey, N. Unique CT emission from aryl terpyridine nanoparticles in aqueous Medium: A combined effect of excited state hydrogen bonding and conformational planarization. *Journal of Photochemistry and Photobiology A: Chemistry* **2023,** *435*.

(24) Sinha, S.; Gaur, P.; Mukherjee, T.; Mukhopadhyay, S.; Ghosh, S. Exploring 1,4-dihydroxyanthraquinone as long-range emissive ratiometric fluorescent probe for signaling Zn(2+)/PO4(3-): Ensemble utilization for live cell imaging. *J Photochem Photobiol B* **2015,** *148*, 181.

(25) Xu, S.; He, M.; Yu, H.; Cai, X.; Tan, X.; Lu, B.; Shu, B. A quantitative method to measure telomerase activity by bioluminescence connected with telomeric repeat amplification protocol. *Anal Biochem* **2001,** *299* (2), 188.

(26) Liang, L. J.; Zhao, X. J.; Huang, C. Z. Zn(II) complex of terpyridine for the highly selective fluorescent recognition of pyrophosphate. *Analyst* **2012,** *137* (4), 953.

(27) Das, P.; Bhattacharya, S.; Mishra, S.; Das, A. Zn(II) and Cd(II)-based complexes for probing the enzymatic hydrolysis of Na4P2O7 by alkaline phosphatase in physiological conditions. *Chem*

Commun (Camb) **2011,** *47* (28), 8118.

(28) Liu, X.; Wang, P.; Fu, J.; Yao, K.; Xue, K.; Xu, K. Turn-on fluorescent sensor for Zinc and Cadmium ions based on quinolone and its sequential response to phosphate. *Journal of Luminescence* **2017,** *186*, 16.

(29) Patra, C.; Bhanja, A. K.; Sen, C.; Ojha, D.; Chattopadhyay, D.; Mahapatra, A.; Sinha, C. Imine-functionalized thioether Zn(ii) turn-on fluorescent sensor and its selective sequential logic operations with H2PO4−, DFT computation and live cell imaging. *RSC Advances* **2016,** *6* (58), 53378.

(30) Das, D. K.; Kumar, J.; Bhowmick, A.; Bhattacharyya, P. K.; Banu, S. 2-Hydroxyacetophenone and ethylenediamine condensed Schiff base: Fluorescent sensor for Al3+ and PO43−, biological cell imaging and INHIBIT logic gate. *Inorganica Chimica Acta* **2017,** *462*, 167.

(31) Halcrow, M. A. The synthesis and coordination chemistry of 2,6-bis(pyrazolyl)pyridines and related ligands — Versatile terpyridine analogues. *Coordination Chemistry Reviews* **2005,** *249* (24), 2880.

(32) Das, P.; Ghosh, A.; Kesharwani, M. K.; Ramu, V.; Ganguly, B.; Das, A. Zn（II） －2,2′:6′,2″－Terpyridine－Based Complex as Fluorescent Chemosensor for PPi, AMP and ADP. *European Journal of Inorganic Chemistry* **2011,** *2011* (20), 3050.

(33) Tsukamoto, T.; Takada, K.; Sakamoto, R.; Matsuoka, R.; Toyoda, R.; Maeda, H.; Yagi, T.; Nishikawa, M.; Shinjo, N.; Amano, S.et al. Coordination Nanosheets Based on Terpyridine-Zinc(II) Complexes: As Photoactive Host Materials. *J Am Chem Soc* **2017,** *139* (15), 5359.

(34) Hsu, T. W.; Fang, J. M. Effective assay of bacterial transglycosylation by molecular turn-on sensing and a second-order scattering effect. *Analyst* **2021,** *146* (19), 5843.

(35) Samanta, D.; Kumar, M.; Singh, S.; Verma, P.; Kar, K. K.; Maji, T. K.; Ghorai, M. K. Triphenylamine and terpyridine–zinc(ii) complex based donor–acceptor soft hybrid as a visible light-driven hydrogen evolution photocatalyst. *Journal of Materials Chemistry A* **2020,** *8* (42), 21968.

(36) Xu, Z.; Ren, Y.-Y.; Fan, X.; Cheng, S.; Xu, Q.; Xu, L. A naphthalimide-based fluorescent probe for highly selective detection of pyrophosphate in aqueous solution and living cells. *Tetrahedron* **2015,** *71* (31), 5055.

(37) SOOK KYUNG KIM, D. H. L., JONG-IN HONG, JUYOUNG YOON. Chemosensors for Pyrophosphate. *January 2009 23-31 ACCOUNTS OF CHEMICAL RESEARCH* **09/18/2008,** *42, No. 1*.

(38) Santos, J. J.; Toma, S. H.; Lalli, P. M.; Riccio, M. F.; Eberlin, M. N.; Toma, H. E.; Araki, K. Exploring the coordination chemistry of isomerizable terpyridine derivatives for successful analyses of cis and trans isomers by travelling wave ion mobility mass spectrometry. *Analyst* **2012,** *137* (17), 4045.

(39) Mei, J.; Leung, N. L.; Kwok, R. T.; Lam, J. W.; Tang, B. Z. Aggregation-Induced Emission: Together We Shine, United We Soar! *Chem Rev* **2015,** *115* (21), 11718.

(40) Zhou, G.; Zhang, X.; Ni, X. L. Tuning the amphiphilicity of terpyridine-based fluorescent probe in water: Assembly and disassembly-controlled H g(2+) sensing, removal, and adsorption of H(2)S. *J Hazard Mater* **2020,** *384*, 121474.

(41) Lin, W.; Xie, X.; Wang, Y.; Chen, J. A New Fluorescent Probe for Selective Cd2+ Detection and Cell Imaging. *Zeitschrift für anorganische und allgemeine Chemie* **2019,** *645* (8), 645.

(42) Ghosh, B. N.; Topic, F.; Sahoo, P. K.; Mal, P.; Linnera, J.; Kalenius, E.; Tuononen, H. M.;

Rissanen, K. Synthesis, structure and photophysical properties of a highly luminescent terpyridine-diphenylacetylene hybrid fluorophore and its metal complexes. *Dalton Trans* **2015,** *44* (1), 254.

(43) Tang, A.; Yin, Y.; Chen, Z.; Fan, C.; Liu, G.; Pu, S. A multifunctional aggregation-induced emission (AIE)-active fluorescent chemosensor for detection of Zn2+ and Hg2+. *Tetrahedron* **2019,** *75* (36).

(44) Sun, X. J.; Liu, T. T.; Li, N. N.; Zeng, S.; Xing, Z. Y. A novel dual-function probe for recognition of Zn(2+) and Al(3+) and its application in real samples. *Spectrochim Acta A Mol Biomol Spectrosc* **2020,** *228*, 117786.

(45) Das, B.; Dolai, M.; Dhara, A.; Ghosh, A.; Mabhai, S.; Misra, A.; Dey, S.; Jana, A. Solvent-Regulated Fluorimetric Differentiation of Al(3+) and Zn(2+) Using an AIE-Active Single Sensor. *J Phys Chem A* **2021,** *125* (7), 1490.

(46) Li, Y.; Gu, Z.; He, T.; Yuan, X.; Zhang, Y.; Xu, Z.; Qiu, H.; Zhang, Q.; Yin, S. Terpyridyl-based triphenylamine derivatives with aggregation-induced emission characteristics for selective detection of Zn2+, Cd2+ and CN− ions and application in cell imaging. *Dyes and Pigments* **2020,** *173*.

(47) Lu, X.; Wu, M.; Wang, S.; Qin, J.; Li, P. An AIE/PET-based fluorescent probe for Zn2+/Al3+ detection and its application in fluorescence-assisted diagnosis for prostate cancer. *Dyes and Pigments* **2022,** *203*.

(48) Gogoi, A.; Mukherjee, S.; Ramesh, A.; Das, G. Nanomolar Zn(ii) sensing and subsequent PPi detection in physiological medium and live cells with a benzothiazole functionalized chemosensor. *RSC Advances* **2015,** *5* (78), 63634.